A Moderate-Affinity Antibody-Drug Conjugate Targeting B7-H3 Exerts Potent Antitumor Efficacy

Ziyu Zhang †, Huifang Zong †, Zhen Li, Shusheng Wang, Xiaodong Xiao *, Yueqing Xie *, Jianwei Zhu *

Posted Date: 9 February 2026

doi: 10.20944/preprints202602.0621.v1

Keywords: antibody-drug conjugate; B7-H3; cancer therapy; solid tumor; developability

Article

A Moderate-Affinity Antibody-Drug Conjugate Targeting B7-H3 Exerts Potent Antitumor Efficacy

Ziyu Zhang [1,†], Huifang Zong [2,†], Zhen Li [2,†], Shusheng Wang [2], Xiaodong Xiao [2,3,*], Yueqing Xie [2,3,*] and Jianwei Zhu [1,2,3,*]

[1] Engineering Research Center of Cell & Therapeutic Antibody, Ministry of Education, China, School of Pharmacy, Shanghai Jiao Tong University, Shanghai 200240, China

[2] Jecho Institute Co., Ltd., Shanghai 200240, China

[3] Jecho Laboratories, Inc., MD 21704, USA

* Correspondence: xiaodong.xiao@jecholabs.com (X.X.); yueqing.xie@gmail.com (Y.X.); jianweiz@sjtu.edu.cn (J.Z.)

† They contributed to this work equally.

Abstract

Background: B7-H3, a type I transmembrane glycoprotein belonging to the B7 superfamily, is an attractive target for antitumor therapies. B7-H3 demonstrates aberrant overexpression in various types of solid tumors while limited and low expression in normal human organs. Various types of treatment targeting B7-H3 have been reported. Among these treatments, antibody-drug conjugate (ADC) has shown potent activity and several clinical trials including DS7300a and MGC018 are currently ongoing. **Methods**: Here, we constructed CD276-8 ADC composed of anti-B7-H3 antibody CD276-8 with moderate affinity, enzymatically cleavable tetra-peptide–based linker and DXd. Characteristics including *in vitro* binding affinity and internalization activity was assessed by Bio-Layer Interferometry (BLI), flow cytometry and high content analysis (HCA). The cytotoxicity of CD276-8 ADC was evaluated by the cell-lines with B7-H3 expressed. Pharmacokinetics profiles and antitumor activity were evaluated in mice models *in vivo*. Finally, developability of CD276-8 ADC was assessed with plasma stability, accelerate stability and freeze-thawing studies using LC-MS and HPLC. **Results**: Characterization *in vitro* demonstrated the moderate affinity and acceptable internalization activity of CD276-8 ADC. In addition, CD276-8 ADC appeared potent antitumor activities in B7-H3-positive cell line-derived xenograft (CDX) models with acceptable pharmacokinetics profiles, although it showed less potent cytotoxicity in various cell lines *in vitro*, indicating acceptable developability. **Conclusions**: We developed CD276-8 ADC, a B7-H3-targeting ADC with moderate affinity, which delivers the TOP1 inhibitor DXd. This design enabled superior tumor penetration and favorable pharmacokinetics, resulting in potent antitumor efficacy *in vivo*. Our study highlights affinity optimization as a crucial strategy for enhancing ADC efficacy, positioning CD276-8 ADC as a promising therapeutic for B7-H3-expressing solid tumors.

Keywords: antibody-drug conjugate; B7-H3; cancer therapy; solid tumor; developability

1. Introduction

B7-H3, also known as CD276, is a type I transmembrane glycoprotein belonging to the B7 superfamily that includes immune checkpoints like PD-L1, B7-1 (CD80) and B7-2 (CD86)[1]. Studies have reported that overexpression of B7-H3 in tumor tissues was correlated with poor clinical prognosis in various types of cancers. Besides, immunohistochemistry (IHC) studies further identify its surface expression on stromal components within the tumor microenvironment (TME), involving fibroblasts, vascular endothelial cells, pericytes and transformed epithelial cells[2,3]. Clinical investigations across multi-institutional cohorts have revealed that B7-H3 demonstrates aberrant overexpression in diverse solid malignancies including non-small cell lung cancer (NSCLC),

 doi:10.20944/preprints202602.0621.v1

pancreatic ductal adenocarcinoma, hepatocellular carcinoma, breast carcinoma, prostate adenocarcinoma, and cutaneous melanoma[2,4–6]. On the other hand, despite the broad expression at the mRNA level in normal human tissues, the protein expression of B7-H3 is limited and remains at relatively low levels in normal human organs such as liver, pancreas, ovary, kidney and prostate[2].

Recent studies suggest that B7-H3 is a coinhibitory molecule inhibiting the activation and proliferation of T-cells[1,7] and promotes pro-tumor functions such as tumor progress, migration, invasion, drug resistance, metabolism, and angiogenesis[8]. Although the physiologic functions of B7-H3 are still incompletely characterized, it is expected to be a novel attractive pan-tumor target for antitumor therapies due to its expression profiles. Various of treatment methods targeting B7-H3 include monoclonal antibodies(mAbs) with enhanced antibody-dependent cellular cytotoxicity (ADCC), T-cell engager (TCE) bispecific antibodies, chimeric antigen receptor (CAR)-T cells, and ADCs have been conducted[3,9].

ADCs are composed of a mAb, linker, and biologically active payload like cytotoxic drugs. They are designed to exert potent antitumor activity against the tumor cells expressing targeted antigen by delivering payload into the cells[10–12]. 19 ADCs have been approved globally and numerous clinical studies of new ADCs are ongoing[10,11]. As for B7-H3, clinical studies of several ADCs targeting B7-H3 like DS7300a, MGC018, YL201 are ongoing[9,13]. GGFG-DXd, a linker-payload technology from Daiichi Sankyo has been confirmed to be stable and potent in previous clinical studies. ADCs using GGFG-DXd lilke T-DXd targeting to HER2 and Dato-DXd targeting to Trop2 have been developed and approved[14,15]. Therefore, we chose GGFG-DXd to prepare ADCs to evaluate the activity of antibodies.

Therefore, we generated CD276-8 ADC, a moderate-affinity B7-H3–targeting ADC, that is composed of a humanized anti–B7-H3 mAb, an enzymatically cleavable tetra-peptide–based linker, and DXd. The ADC is designed to bind to B7-H3 on the cell surface and release DXd in cytoplasm after being internalized into cell and being cleaved in lysosomes by enzymes. The released DXd inhibits TOP1 activity and leads to the apoptosis of target cancer cells. Here, we demonstrate preclinically that CD276-8 ADC is well capable of inhibiting tumor growth or regressing tumor volume in multiple B7-H3 positive models. Further, our studies including pharmacokinetic (PK) and *in vitro* stability assessment of CD276-8 ADC suggests its safety and druggability. Taken together, these studies indicate that CD276-8 ADC has the potential to be a promising ADC for solid tumor malignancies.

2. Materials and Methods

2.1. Antibodies and ADCs

The parental anti-B7-H3 antibodies (Ab) CD276-3 and CD276-8, humanized IgG1 mAb, were generated by phage display technology. The CDR sequences of DS7300a parental antibody[16] (described as DS7300 in this study) were from US11633493B2[17] and its structure is the same as parental anti-B7-H3 antibodies. The DS7300 was used as a positive control in the study.

To produce CD276-3 ADC, CD276-8 ADC, DS7300 ADC and isotype ADC control with an average DAR of 8, antibodies with native cysteine residues was conjugated to the linker-payload composed of DXd and a maleimide-GGFG peptide by a standard method[11,18]. In addition, DS7300 ADC with an average DAR of 4 were produced with the existence of transition metal ion Zn^{2+} to improve the homogeneity of ADC[19]. The purities of antibodies and ADCs were characterized by size exclusion chromatography (SEC-HPLC). The DAR of ADCs were detected by RP-HPLC using a method in previous reports using ultrapure water and acetonitrile with 0.1% trifluoroacetic acid (TFA) as mobile phase A and B[20]. The DAR of each ADC was calculated with the formular:

$$DAR=2\times (\Sigma_{\text{LC Weighted peak area}} + \Sigma_{\text{HC Weighted peak area}})/100$$

 doi:10.20944/preprints202602.0621.v1

2.2. Cell Lines

The human glioma cell line U251 (RRID: CVCL_0021), the human gastric carcinoma cell NCI-N87 (RRID: CVCL_1603), the human ovarian carcinoma cell OVCAR3 (RRID: CVCL_0465), and the human pancreatic adenocarcinoma cell BxPC-3 (RRID: CVCL_0186) were purchased from ATCC. The human epidermoid carcinoma cell A431 (RRID: CVCL_0037) and the human lung adenocarcinoma cell HCC827 (RRID: CVCL_2063) were purchased from Hysigen Bioscience (Suzhou, China). The human ovarian teratoma cell PA-1 (RRID: CVCL_0479) were purchased from Procell Life Science&Technology Co., Ltd. (Wuhan, China). The human melanoma cell line A375 (RRID: CVCL_0132), the human breast cancer cells, MCF-7 (RRID: CVCL_0031), MDA-MB-231 (RRID: CVCL_0062), the human liver hepatocellular carcinoma cells, HepG2 (RRID: CVCL_0027), Huh7 (RRID: CVCL_0336), the human Burkitt's lymphoma cells, Raji (RRID: CVCL_0511), Daudi (RRID: CVCL_0008) were kept in Jecho Institue Co., Ltd. (Shanghai, China). All of the cells were cultured with appropriate media.

2.3. B7-H3 Expression Analysis by Fluorescence Activated Cell Sorting (FACS)

Each cell line was treated with DS7300 or human IgG1 isotype control, and was stained with PE-conjugated F(ab')2-goat anti-human IgG Fc (Invitrogen). Each sample was analyzed by Attune NxT (ThermoFisher), and the expression of cell surface B7-H3 was evaluated in forms of mean fluorescence intensity (MFI) folds in comparison with Isotype control.

2.4. Bio-Layer Interferometry Assay

The binding affinities and avidities of CD276-3, CD276-8 and DS7300 with recombinant human B7-H3 (rhB7-H3) protein (4Ig B7-H3, His tag) (Sino Biological, Inc. Beijing, China) were analyzed by BLI with Gator PRIME (Gator Bio, Shanghai, China). RhB7-H3 protein with His tag was immobilized to Ni NTA probe (Gator Bio) and was associated to CD276-3, CD276-8 or DS7300 for antibody avidity analysis.

Further, epitope grouping of CD276-3, CD276-8 and DS7300 was processed. RhB7-H3 protein was immobilized to Ni NTA probe and was associated to CD276-3, CD276-8 or DS7300. After first antibody association, the probe was associated with CD276-3, CD276-8 or DS7300 separately. The binding response of each mAb was determined as Ab1 and Ab2 to obtain Shift 1 (nm) and Shift 2 (nm), and the inhibition rates of Ab1 against Ab2 were calculated with 100%×(1-(Shift 2 of Ab1 with Ab2 as first antibody)/(Shift 1 of Ab1)).

2.5. Cell Binding Affinity Alysis

The binding affinity against cell surface antigen of CD276-3, CD276-8 or DS7300 was evaluated by FACS. U251 or A375 cells were seeded into 96-well cell culture plates at a concentration of 1.5×10^5 cells per well. CD276-3 CD276-8, DS7300 or human IgG isotype control was serial diluted and incubated with cells for 30 minutes at 4 ℃. Then the cells were washed and incubated with PE-conjugated F(ab')2-goat anti-human IgG Fc for 30 minutes at 4℃. After washing and resuspension, samples were analyzed by Attune NxT. The EC_{50} value calculated in GraphPad Prism using a nonlinear, 4-parameter curve fit model to calculate the binding affinity against cell surface B7-H3 of CD276-3, CD276-8 and DS7300.

2.6. Cell Internalization Evaluation

Internalization of CD276-3, CD276-8 or DS7300 was evaluated by FACS. U251 cells were seeded into 96-well cell culture plates at 1×10^4 cells per well, and incubated overnight at 37℃ in a humidified atmosphere containing 5% CO2. CD276-3, CD276-8, DS7300 or human IgG isotype control was mixed with pHrodo iFL Green (Invitrogen), and then incubated with cells at 37 ℃ for 24 hours (h) in a humidified atmosphere containing 5% CO_2. The internalization condition was detected with standard FITC using Attune NxT.

 doi:10.20944/preprints202602.0621.v1

Further, antibodies conjugated with pHrodo Red (Invitrogen) was visualized in cell plasma by HCA. OVCAR3 cells (1×10^4 cells/well) were dosed with 0.1 mg/mL antibodies conjugated with pHrodo Red at 37 ℃ for 4 h. Treated cells were washed with PBS to remove unbound antibodies. In addition to the signal of antibody-pHrodo, treated cells were visualized with Lysosensor Green (Invitrogen) and Hoechst Blue[21]. The stained cells were detected by Operetta CLS (Perkin Elmer), and the co-positioning situation was analyzed using ImageJ_JoCAP.

2.7. In Vitro Cytotoxicity

Cells were seeded into 96-well cell culture plates at 500 to 2000 cells per well. After overnight incubation at 37 ℃, each serial diluted substance (CD276-3 ADC, CD276-8 ADC, DS7300 ADC (DAR8) and isotype ADC control) was added and then all the plates were incubated for 5 days. After incubation, cell viability was detected by SpectraMax iD5 (Molecular Devices, LLC.) using CellTiter-Glo (CTG, Promega Corp.) The half maximal inhibitory concetration (IC_{50}) of each substance was calculated in GraphPad Prism using a nonlinear, 4-parameter curve fit model.

2.8. In Vivo Activity

All animal experiments performed in this study were reviewed and approved by the Institutional Animal Care and Use Committees of Laboratory Animal Center, Shanghai Jiao Tong University.

2.8.1. PK Study in Mice

CD276-3 ADC or CD276-8 ADC was injected once intravenously at 5 mg/kg to female NU/NU mice. Serum concentration of ADC, total antibody (drug conjugated and unconjugated antibody), and DXd were measured up to 21 days post treatment. Concentrations of total antibody and ADC were detected by ELISA[22], and DXd were detected by LC-MS[23]. Below lower limit of quantification (BLQ) for ADC and total antibody: 0.137 ug/mL, and BLQ for DXd: 0.1 ng/mL. The pharmacokinetic parameters were calculated by noncompartmental analysis with PKSolver 2.0[24].

2.8.2. Tumor Inhibitory in Cancer Cell Line-Derived Xenograft Models

A375, Huh7 and OVCAR3 models were established by injecting 5×10^6 cells suspended in RPMI 1640, while PA-1 model was established by injecting 9×10^6 cells suspended in RPMI 1640, subcutaneously into female NU/NU mice (Vital River Laboratory Animal Technology Co., Ltd., Zhejiang, China).

When the tumor volume reached approximately 100-300 mm^3, mice were randomly distributed into study groups. Mice bearing tumor were treated with CD276-3 ADC, CD276-8 ADC, DS7300 ADC (DAR4 or DAR8), or Isotype ADC control intravenously on days 0. Mice in Huh7 model were treated with a second dose on days 14. The tumor volume and weight were measured twice a week, and the tumor volume was defined as 0.5 × tumor length × tumor $width^2$. The antitumor activity was evaluated when the tumor volume of Isotype ADC control group reached 2000 mm^3 (1000 mm^3 in case of PA-1 and OVCAR3 models). In addition, the tumor growth inhibition (TGI, %) was calculated with the formula:

$$TGI=100 \times (1- (V_T)/(Vc))$$

V_T: average tumor volume of treatment group
Vc: average tumor volume of control group

 doi:10.20944/preprints202602.0621.v1

2.9. Developability Assessment of the ADC

2.9.1. Characterization of CD276-8

The purity and colloidal stability of CD276-8 was characterized using standup monolayer adsorption chromatography (SMAC-HPLC)[25], while nonspecific interaction using cross interaction chromatography (CIC-HPLC) compared with Tremelimumab[26]. In addition, the thermal stability of CD276-8 was characterized by Differential Scanning Fluorimetry (DSF) in the form of melting point (T_m).

2.9.2. Stability of CD276-8 and CD276-8 ADC in Forced Degradation

Accelerated stability (AS) and freeze-thawing (F/T) stability of CD276-8 were evaluated by forced degradation of CD276-8. CD276-8 in phosphate buffered saline (PBS, pH 5.5) was either in a 40 ℃ water bath for 14 days or in freezer with frozen at -80 ℃. The frozen samples were thawed at 25 ℃ for 5 cycles. The aggregation of each sample was characterized by SEC-HPLC. And the charge variants were detected by weak cation exchange chromatography (WCX-HPLC) using 20 mM MES buffer (pH 6.7, phase A) and 20 mM MES buffer (pH 6.7, 0.5 M NaCl, phase B) as mobile phase with a linear gradient of 5-50% phase B from 3 minutes to 30 minutes and 80% phase B from 30 minutes to 40 minutes.

CD276-8 ADC in histidine buffer (pH 5.5) was treated either in 25 ℃ water bath or 5 freeze and thaw cycles in temperature 25 ℃ to -80 ℃ to assess the stability under the condition. For each sample the aggregation was detected by SEC-HPLC, the DAR of CD276-8 ADC was detected by RP-HPLC using a method in previous reports using ultrapure water and acetonitrile with 0.1% trifluoroacetic acid (TFA) as mobile phase A and B[20]. In case of ADC biological activities, the cell binding affinity and in vitro cytotoxicity changes between samples were measured by FACS and SpectraMax iD5 using OVCAR3 cells.

2.9.3. In Vitro Plasma Stability of CD276-8 ADC

CD276-8 ADC was diluted into human, monkey and mouse plasma to yield a final solution with 0.2 mg/mL CD276-8 ADC and the sample was incubated at 37 ℃. Plasma concentration of DXd and DAR of CD276-8 ADC were measured up to 14 days by LC-MS[23]. The BLQ for DXd was 0.1 ng/mL.

3. Results

3.1. Expression of B7-H3 in Cancer Cell Lines

To investigate the cell surface expression of B7-H3 in cell lines, we conducted FACS analysis (Figure 1a) and most solid tumor cell lines analyzed displayed high B7-H3 positive signals, showing high MFI fold over 20 folds. In contrast, lymphoma cell lines like Raji and Daudi were determined negative. The results of FACS indicated the high expression of B7-H3 in various types of solid tumors but not in hematological cancer including leukemia, lymphoma and myeloma, consistent with datasets from the Human Protein Atlas (HPA) dataset and previous studies[2,4–6].

3.2. Characterization of Parental Antibodies CD276-3 and CD276-8

We generated CD276-3 and CD276-8 targeting to human B7-H3 as candidate antibodies in order to obtain an anti-B7-H3 ADC for anti-cancer studies. The binding affinity against recombinant human B7-H3 (rhB7-H3) (4Ig) was assessed by BLI, and the K_D of CD276-3, CD276-8 and DS7300 were 1.24 nM, 2.12 nM and 0.231 nM (Table 1, Figure S1). The cell surface binding affinity was detected in U251 and A375 (Figure 1b, c), and the affinity results were 37.32 nM, 7.246 nM for the EC_{50} of CD276-3, CD276-8 in U251, and 29.60 nM, 3.115 nM for the EC_{50} of CD276-3, CD276-8 in A375, while DS7300 appeared higher affinity with an EC_{50} of 2.981 nM in U251 and 1.452 nM in A375. Both candidates demonstrated moderate binding affinity with lower span and higher EC_{50} compared with DS7300.

 doi:10.20944/preprints202602.0621.v1

Further, the epitope grouping of CD276-3, CD276-8 and DS7300 was analyzed by BLI (Figure S2a). A heatmap was generated according to the inhibition between candidates, demonstrating that CD276-3 shared a similar binding epitope to DS7300 while CD276-8 bound to a different epitope (Figure S2b).

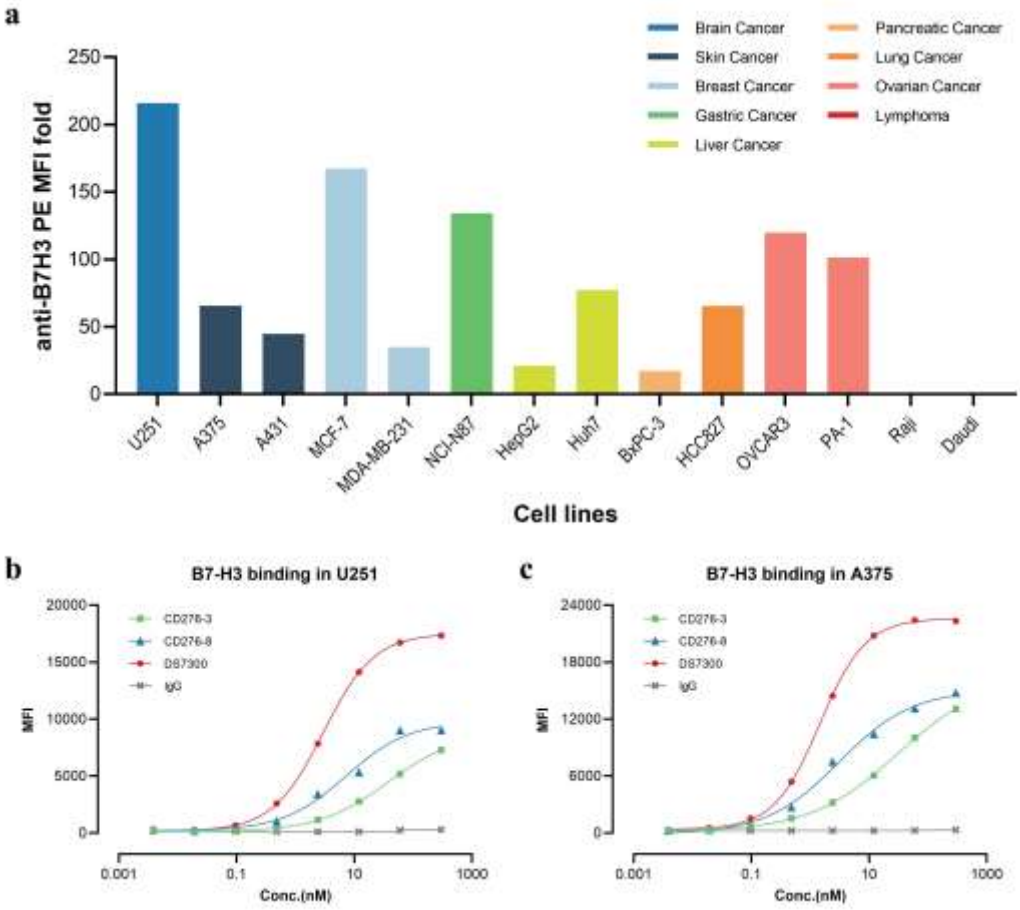

Figure 1. Expression of B7H3 in cell lines and *in vitro* binding affinity of CD276-3, CD276-8 and DS7300. **(a)** Cell surface expression of B7H3 in cell lines, as determined by FACS. Different colors represent different types of cancer. Cell surface binding affinity of CD276-3, CD276-8 and DS7300 against B7-H3 in U251 **(b)** and A375 **(c)** cells, as determined by FACS.

Table 1. Binding affinity against rhB7-H3 (4Ig) of CD276-3, CD276-8 and DS7300 as determined by BLI.

Antibody	K_{off} (1/s)	K_{on} (1/Ms)	K_D (nM)
CD276-3	1.74×10^{-3}	1.41×10^{6}	1.24
CD276-8	7.02×10^{-4}	3.31×10^{5}	2.12
DS7300	2.35×10^{-4}	1.02×10^{6}	0.231

Considering that antibody for ADC construction requires a high internalization activity to deliver the payload into tumor cells, the internalization activity of candidates was assessed *in vitro*. Candidate antibodies and DS7300 were labeled with pHrodo Green and incubated with U251 cells for 24 h (Figure 2a). The labeled antibodies fluoresced green when pH decreased and was detected using FACS, indicating that the antibodies were internalized into cells. Although CD276-8 showed moderate affinity compared to DS7300, it demonstrated better internalization activity than DS7300. Epitope difference may contribute to the internalization of CD276-8. In addition, the internalization activity of candidates was visually assessed in OVCAR3 using HCA (Figure 2b). After 4 h of incubation, the red staining was observed intracellularly indicating colocalization of antibodies with

 doi:10.20944/preprints202602.0621.v1

the green-stained lysosomes, indicating that mAbs may be delivered through lysosomes intracellularly after receptor-mediated internalization.

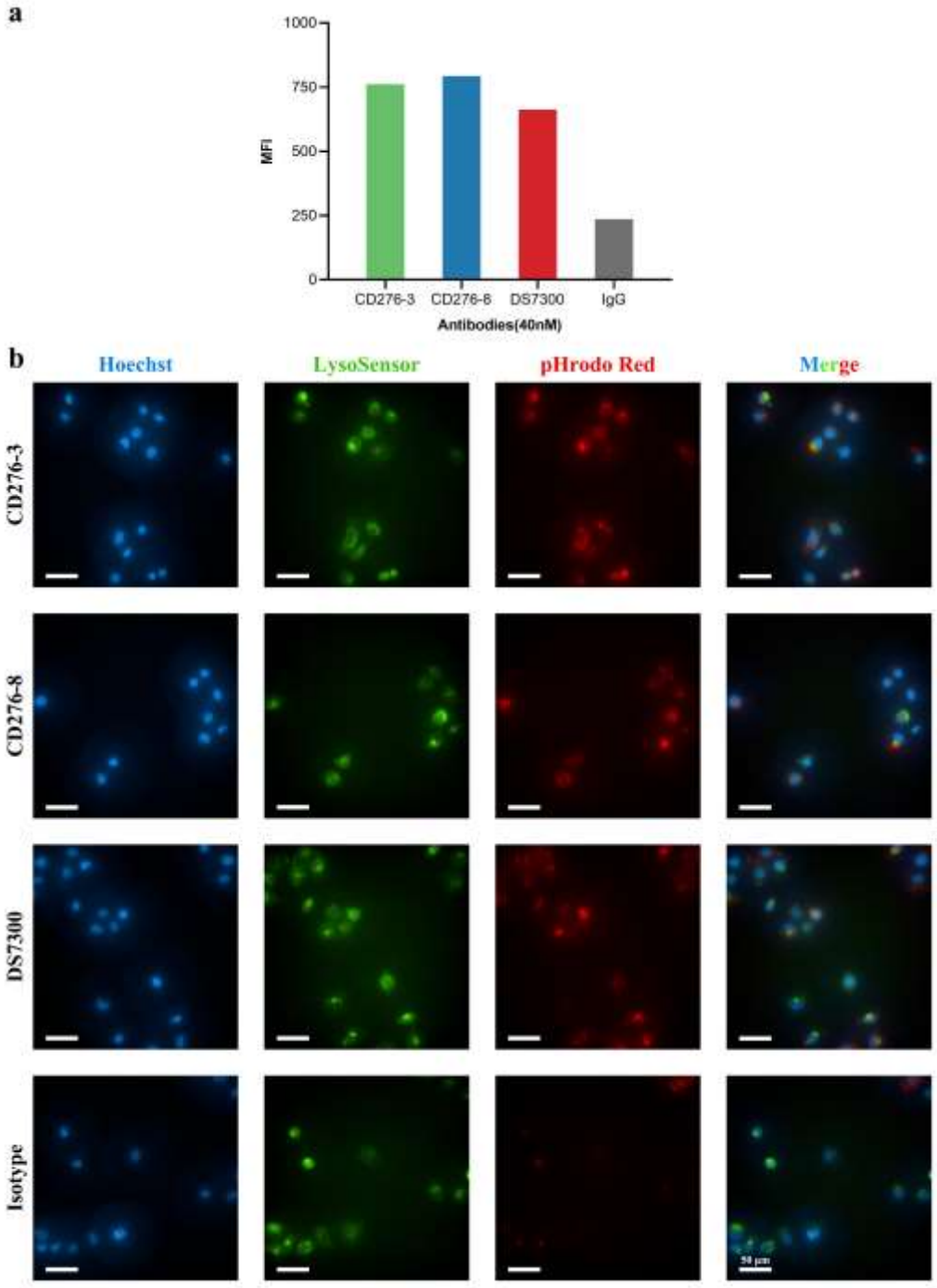

Figure 2. Internalization activity of CD276-3, CD276-8 and DS7300. Internalization assessment of CD276-3, CD276-8 and DS7300 **(a)** in U251 cells by FACS, **(b)** in OVCAR3 by HCA.

3.3. In Vitro Cytotoxicity of CD276-3 ADC, CD276-8 ADC and DS7300 ADC (DAR8)

After characterization, DAR8 ADCs including CD276-3 ADC, CD276-8 ADC, DS7300 ADC and Isotype ADC were generated by conjugating mc-GGFG-DXd and native cysteine residues of antibodies, while DS7300 ADC (DAR4) was generated by conjugating cysteine residues between light chain and heavy chain of antibody and mc-GGFG-DXd (Figure 3a). The purity of each ADC and

 doi:10.20944/preprints202602.0621.v1

antibody was detected by SEC-HPLC and no clear differences between the antibodies and ADCs was observed (Δpurity≤3%) as shown in Figure S3. The DARs of each ADC were detected by RP-HPLC. The DARs of DAR8 ADCs ranged from 7.26 to 7.56, and the DAR of DS7300 ADC (DAR4) was 4.42, meeting the expectation DAR values (Figure S3) as designed.

The *in vitro* cytotoxicity of DAR8 ADCs was evaluated using several cell lines, and the IC_{50} values were concluded in Table 2. The IC_{50} of ADCs were varies widely depend on cell surface B7-H3 expression as shown in Figure 1a. In B7-H3 positive expression cell lines, such as A375, Huh7, OVCAR3 and PA-1, all three ADCs showed specific tumor cell-killing (Figure 3b-e). In cells without B7-H3 expression like Raji, no clear differences in IC_{50} were observed for all the ADCs (Table 2), indicating CD276-3 ADC and CD276-8 ADC exerted no B7-H3-specific cytotoxicity in negative cells. These results demonstrated that CD276-3 ADC and CD276-8 ADC showed B7-H3 depended cytotoxicity *in vitro*, with CD276-3 ADC showing better activity. However, some types of cancer cells were not sensitive to B7-H3 ADCs even though the cells expressed B7-H3 as detected by FACS (Table 2). The mechanisms causing the large differences in sensitivity could be related to cell-type-specific variations in target-mediated internalization, mitotic index, driver mutations, DNA repair capacity, apoptotic sensitivity, drug trafficking, drug metabolism, or efflux[13]. These findings suggested that *in vitro* sensitivity screening could serve as a valuable approach for identifying cancer types sensitive to DXd-containing ADCs, aiding personalized therapy and helping ensure an optimal therapeutic window for DXd-containing ADCs[13].

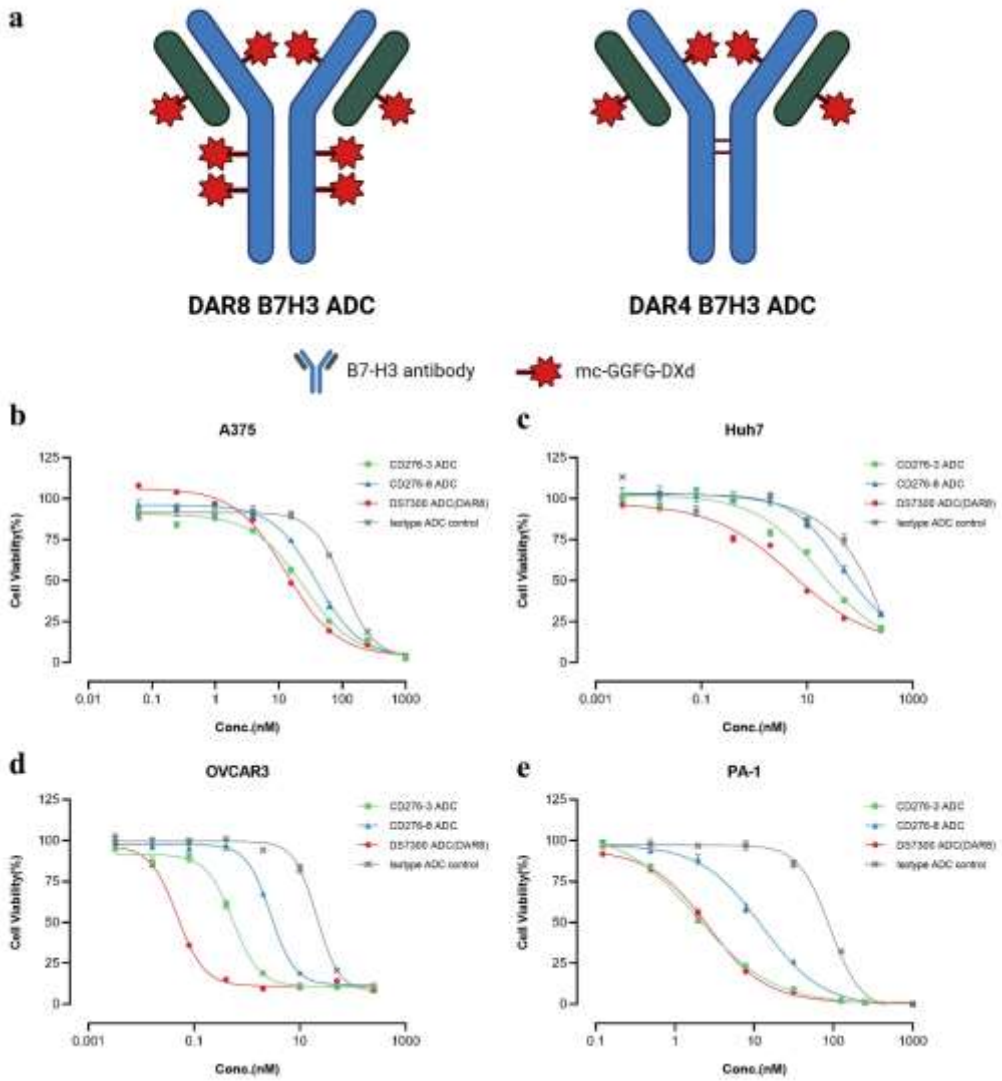

 doi:10.20944/preprints202602.0621.v1

Figure 3. Structure of DAR8 and DAR4 ADCs and In vitro cytotoxicity of CD276-3 ADC, CD276-8 ADC and DS7300 ADC (DAR8). **(a)** Chemical Structure of DAR8 and DAR4 ADCs. The *in vitro* cytotoxicity was determined in positive cell lines including A375 **(b)**, Huh7 **(c)**, OVCAR3 **(d)**, PA-1 **(e)**. Each value was represented the mean and standard error of mean (SEM).

Table 2. *In vitro* cytotoxicity (IC_{50}) of ADCs in various cell lines.

Cell line	Cancer type	IC_{50} (nM)			
		CD276-3 ADC	CD276-8 ADC	DS7300 ADC (DAR8)	Isotype ADC
Raji	lymphoma	51.99	52.14	55.13	61.31
U251	Glioma	> 200	> 200	> 200	> 200
A375	melanoma	23.91	38.67	12.97	104.1
A431	skin cancer	176.7	> 200	> 200	> 200
MDA-MB-231	breast cancer	> 200	> 200	> 200	> 200
NCI-N87	stomach cancer	> 200	> 200	> 200	> 200
HepG2	liver cancer	> 200	> 200	> 200	> 200
Huh7	liver cancer	17.39	43.69	5.265	> 200
HCC827	lung cancer	21.73	15.04	7.746	38.72
OVCAR3	ovarian cancer	0.539	2.802	0.048	20.73
PA-1	ovarian teratoma	1.897	12.43	2.613	89.76

*The ADC are considered no specific cytotoxicity in a cell line when the IC_{50} exceeded 200 nM or similar to Isotype ADC control.

3.4. Pharmacokinetics of the ADCs in Mice

CD276-3 ADC or CD276-8 ADC was administered once intravenously at 5 mg/kg to mice. Then serum concentrations of ADC, total antibody and DXd were determined up to 21 days post injection. The terminal elimination half-times ($t_{1/2}$) of CD276-3 ADC and CD276-8 ADC were 3.96 and 9.66 days respectively, while the $t_{1/2}$ of CD276-3 total antibody and CD276-8 total antibody were 5.76 and 11.65 days (Figure 4; Table 3). CD276-8 ADC showed a longer half-time (Figure 4; Table 3) and had the potential for long-last and potent tumor growth inhibition *in vivo*. Additionally, low serum concentrations of DXd were detected (Figure 4), indicating low systemic exposure to DXd attributed to the stable linker of CD276-3 ADC and CD276-8 ADC in comparison to previous reports[27–29]. Further, no increase of the DXd concentration was observed even though CD276-8 ADC had a longer half-time, indicating a considerable safety in mice (Figure 4).

Table 3. Pharmacokinetic parameters of CD276-3 ADC and CD276-8 ADC in mice.

PK parameter	CD276-3 ADC	CD276-3 Total Ab	CD276-8 ADC	CD276-8 Total Ab
AUC_{inf}(μg·day/mL)	152.03	194.36	260.68	422.64
AUC_{21d}(μg·day/mL)	147.64	179.54	211.45	317.23
CL(mL/day/kg)	32.89	25.72	19.18	11.83
$t_{1/2}$(day)	3.96	5.76	9.66	11.65
V_{ss}(mL/kg)	162.58	185.76	229.86	173.81
MRT_{inf}(day)	4.94	7.22	11.98	14.69

*The parameters were calculated by noncompartmental analysis with PKSolver.

 doi:10.20944/preprints202602.0621.v1

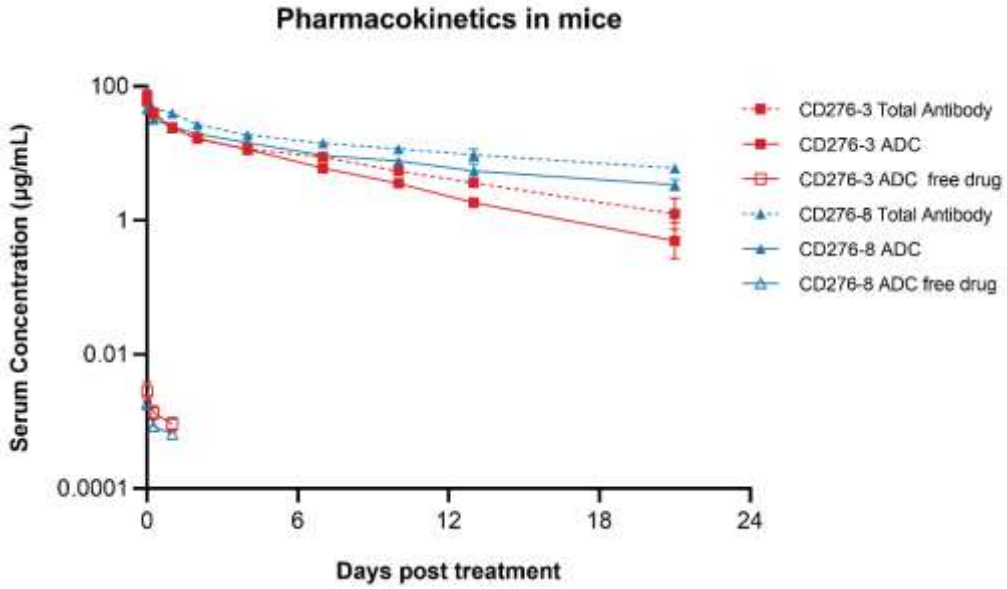

Figure 4. Pharmacokinetics of CD276-3 ADC and CD276-8 ADC in mice. CD276-3 ADC or CD276-8 ADC was administered once intravenously at 5 mg/kg to mice. Serum concentrations of ADC, total antibody and DXd were determined. Each value was represented the mean and SEM (N=5 mice per group).

3.5. Antitumor Activities of the ADCs In Vivo

Antitumor activities of CD276-3 ADC, CD276-8 ADC DS7300 ADC (DAR4) and DS7300 ADC (DAR8) were evaluated using CDX mouse models *in vivo*. CD276-8 ADC demonstrated potent antitumor activities (Figure 5a-e). In the PA-1 model (N=6), 2 mg/kg candidates were compared with DS7300 ADC (DAR8) and DS7300 ADC (DAR4). CD276-8 ADC induced more potent inhibition than CD276-3 ADC and DS7300 ADC (DAR4), with a TGI of 93.1% compared to isotype ADC at 32 days, and 2 of 6 maintaining complete tumor inhibition until the end study (Figure 5a). However, DS7300 ADC (DAR8) demonstrated slight dominance compared to CD276-8 ADC, reaching a TGI of 99.8%.

Further the antitumor activities of CD276-3 ADC, CD276-8 ADC and DS7300 ADC (DAR8) were determined at different dose in A375 and Huh7 CDX mouse models (N=6). In A375 model, CD276-8 ADC induced dose-dependent tumor antitumor activity with TGIs of 94.3% (1 mg/kg) and 100% (3 mg/kg), while the TGIs of DS7300 ADC (DAR8) were 73.7% (1mg/kg) and 99.3% (3 mg/kg) (Figure 5b,c). In Huh7 model, CD276-8 ADC demonstrated durable tumor regression out to day 30, and DS7300 ADC (DAR8) showed a tumor inhibition activity with comparable durability and potency (Figure 5d). Finally, CD276-8 ADC was chosen as the ultimate ADC molecule. And it was further determined its antitumor activity in OVCAR3 model, in which it also showed potent tumor inhibition with a TGI of 69.4% at day 42 (Figure 5e). The body weight of the mice treated with CD276-8 ADC in all models showed no obvious reduction, indicating an *in vivo* safety in mouse models (Figure 5a-e).

Taken together, these results suggest that CD276-8 ADC induced a potent and long-lasting antitumor activity comparable to DS7300 ADC (DAR8). While CD276-3 ADC appeared weaker *in vivo*, although it demonstrated potent cytotoxicity *in vitro*. Therefore, CD276-8 ADC was chosen as the ultimate ADC molecule for further development.

 doi:10.20944/preprints202602.0621.v1

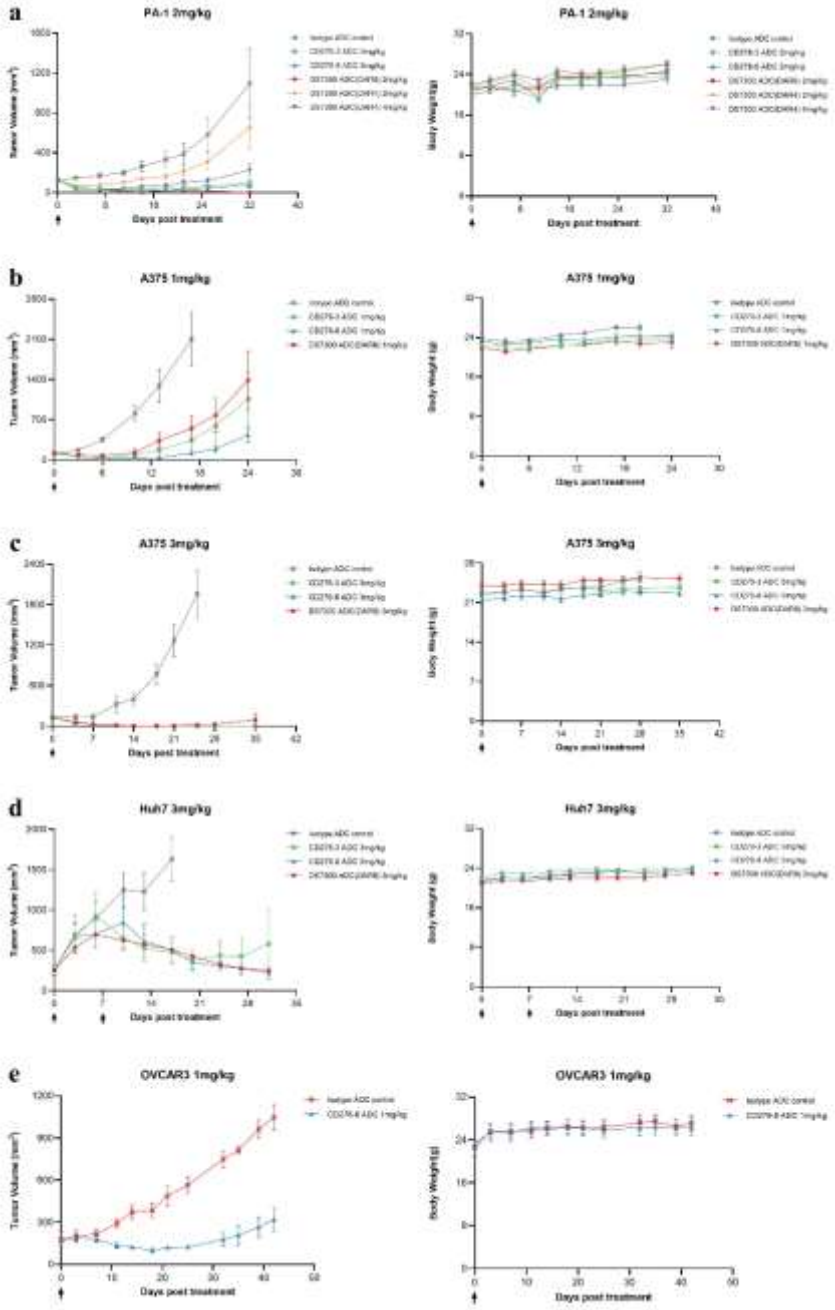

Figure 5. Antitumor activity of CD276-3 ADC, CD276-8 ADC and DS7300 ADC (DAR4 and DAR8) in CDX mouse models *in vivo*. **(a)** Mice with PA-1 cells were treated with CD276-3 ADC, CD276-8 ADC, DS7300 ADC (DAR4), DS7300 ADC (DAR8) or isotype ADC control once. **(b), (c)** Mice with A375 cells were treated once with CD276-3 ADC, CD276-8 ADC, DS7300 ADC (DAR8) or isotype ADC control at 1 mg/kg **(b)** or 3 mg/kg **(c)**. **(d)** Mice with Huh7 cells were treated with CD276-3 ADC, CD276-8 ADC, DS7300 ADC (DAR8) or isotype ADC control at 3 mg/kg at day 0 and day 7. **(e)** Mice with OVCAR3 were treated once with CD276-8 ADC or isotype ADC control. Body weight change of mice was shown for each study at right. Each value was represented the group mean and SEM.

3.6. Developability Assessment of CD276-8 ADC

After comparisons between CD276-3 ADC and CD276-8 ADC *in vivo* and *in vitro*, developability of CD276-8 ADC was assessed.

 doi:10.20944/preprints202602.0621.v1

The parental antibody CD276-8 was characterized to evaluate the colloidal stability and nonspecific interaction compared to a standard sample Tremelimumab[25]. CD276-8 showed a shorter retention time (RT) of 8.992 min in SMAC-HPLC and 8.355 min in CIC-HPLC, while the RT of Tremelimumab was 21.129 min in SMAC-HPLC and 13.088 min in CIC-HPLC, demonstrating low risk of colloidal stability and low nonspecific interaction[25,26] (Figure S4a,b). Further, AS and F/T stability of CD276-8 were analyzed by SEC-HPLC and WCX-HPLC. No clear purity change was observed by SEC-HPLC, demonstrating low aggregation of CD276-8 (Figure S4c). Low ratio of acidic peak of CD276-8 was observed by WCX-HPLC and around 10% of acidic variant was detected after 14 days of incubation at 40 ℃ (Figure S4d), which demonstrated CD276-8 low risk of charge heterogeneity[30]. The T_m of CD276-8 detected by DSF was 68.8 ℃ (Figure S4e), showing acceptable thermal stability[31]. These data indicated that CD276-8 is a stable antibody with good developability.

Further, the T_{m1} and T_{m2} of CD276-8 ADC was examined as 69.8 ℃ and 56.6 ℃ respectively (Figure S4f). Considering the interchain disulfide bonds of CD276-8 were reduced for linker-payload conjugation, the thermal stability change was acceptable. Plasma stability was evaluated *in vitro* in forms of DAR change and DXd release rate in plasma of human, monkey and mouse. The DAR change rates of 0.2 mg/mL CD276-8 ADC after 14 days of incubation in human, monkey and mouse plasma was 34.4%, 64.7% and 40.4% (Figure 6a). And the DXd release rate of CD276-8 ADC after 14-day incubation in human, monkey and mouse plasma was 0.65%, 7.02% and 0.85% (Figure 6b). The stability profiles of CD276-8 ADC were similar to the previously reported ADC using GGFG-DXd[23,32]. In case of forced stability of CD276-8 ADC, structural stability and biological activity were evaluated. No significant alterations were observed in purity and DAR (Figure 6c,d), indicating CD276-8 ADC was stable after 14 days of incubation at 25℃ or 5 cycles of freezing and thawing. The EC_{50} of cell binding affinity and the IC_{50} of *in vitro* cytotoxicity of CD276-8 ADC showed no significant decreasing under the stability testing, further confirming its stability *in vitro*. Taken all data together, CD276-8 ADC shows outstanding developability and is worth for further development.

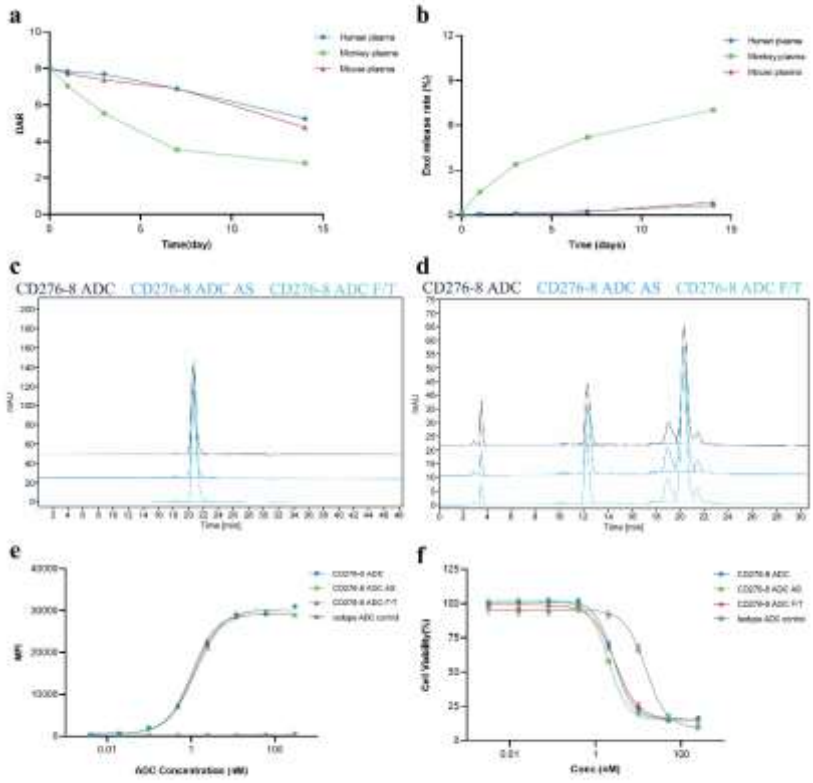

Figure 6. Developability of CD276-8 ADC. **(a,b)** DAR change and DXd release rate of CD276-8 ADC in various types of plasma after incubation up to 14 days, as detected by LC-MS. **(c)** Purity of CD276-8 ADC sample from

 doi:10.20944/preprints202602.0621.v1

AS or F/T study was assessed by SEC-HPLC. **(d)** DAR of CD276-8 ADC sample from AS or F/T study was assessed by RP-HPLC. **(e)** Binding affinity of CD276-8 ADC sample from AS or F/T study was determined using OVCAR3 cells by FACS. **(f)** Cytotoxicity of CD276-8 ADC sample from AS or F/T study was determined using OVCAR3 cells by SpectraMax iD5.

4. Discussion

Here, we report the development of CD276-8 ADC, a potent DXd-based ADC with moderate affinity targeting B7-H3. CD276-8 ADC demonstrated potent and long-lasting antitumor activities in B7-H3-positive CDX models although showing less potent cytotoxicity *in vitro* compared with DS7300 ADC and CD276-3 ADC.

B7-H3, the target of CD276-8 ADC, is a membrane protein with low level of expression on normal human tissues but with higher levels of expression on various of solid tumors including NSCLC, pancreatic cancer, hepatocellular carcinoma, breast carcinoma, prostate adenocarcinoma, and melanoma[2,4–6]. The expression pattern with unmet clinical need indicates that B7-H3 is a promising target for ADC therapy with potential potent antitumor activities and minimal non-specific systemic toxicity.

Compared with CD276-3 ADC and benchmark molecule DS7300 ADC (DAR8), CD276-8 ADC showed a moderate binding affinity against B7-H3 and a weaker cytotoxicity in various B7-H3-positive cell lines *in vitro*. As expected, CD276-8 ADC showed no B7-H3-specific cytotoxicity in B7-H3 negative cells like Raji. Although all of the tested cells were positive to the free payload DXd, CD276-8 ADC could exhibit target-specific cytotoxicity only in some types of tumor cells but no target-specific cytotoxicity in others. The mechanisms causing significant differences in sensitivity could be related to cell-type-specific variations in target-mediated internalization, mitotic index, driver mutations, DNA repair capacity, apoptotic sensitivity, drug trafficking, drug metabolism, or efflux[13]. These results suggested the value of *in vitro* sensitivity screening as a tool for identifying cancer types sensitive to DXd-containing ADCs and ensuring an optimal therapeutic window for DXd-containing ADCs[13].

A pivotal finding of our study was the inconsistency between *in vitro* and *in vivo* activities, highlighting a non-linear relationship between affinity and overall ADC efficacy including *in vitro* cytotoxicity, PK profiles and *in vivo* antitumor activity. Although CD276-8 ADC exhibited a moderate binding affinity and correspondingly weaker cytotoxicity in monolayer cell cultures compared to CD276-3 ADC and high affinity benchmark DS7300 ADC (DAR8), it achieved superior or comparable tumor regression *in vivo*. CD276-8 ADC showed acceptable pharmacokinetic profile in mice with a respectively long half-time and low DXd exposure in serum, which allowed CD276-8 ADC to exert antitumor activity longer but cause low additional systemic toxicity. This discrepancy can be attributed to several advantages conferred by a moderate-affinity antibody in the complex *in vivo* environment. Excessively high affinity can impede the deep penetration of antibodies into solid tumors due to “binding site barrier” effect, where molecules become trapped on the periphery of the tumor mass. The moderate affinity of CD276-8 ADC likely facilitates better distribution throughout the tumor, ensuring the cytotoxic payload reaches a larger proportion of cancer cells, including those in poorly perfused regions[33,34]. And this improved penetration can also maximize the bystander effect, thereby conferring superior efficacy against heterogeneous tumors[35]. Besides, excessively high affinity may lead to premature ADC internalization and degradation in off-target tissues expressing B7-H3, thereby reducing the effective drug payload delivered to the tumor site. In contrast, a moderate affinity can reduce this non-specific binding and internalization without compromising target specificity, optimizing the accumulation of ADC in tumor[33]. Another additional advantage of a moderate-affinity ADC lies in its ability to overcome intratumoral heterogeneity in B7-H3 expression[36]. The reversible binding kinetics not only facilitate uniform drug distribution across tumor cells of diverse antigen density but also enhance tissue penetration[33]. Considering *in vivo* antitumor activity and PK profiles to be paramount, we finally chose CD276-8 ADC to be the ultimate

 doi:10.20944/preprints202602.0621.v1

ADC molecule.The combination of potent *in vivo* efficacy, favorable PK profiles and acceptable developability positions CD276-8 ADC as a promising clinical candidate.

In summary, we developed a potent B7-H3-targeting ADC conjugated with the potent TOP1 inhibitor DXd, CD276-8 ADC. This design enables effective target binding and internalization while promoting superior tumor penetration and a favorable pharmacokinetic profile, which collectively translate into profound antitumor activity *in vivo*. Our findings provide a rationale that may inform future ADC design strategies, suggesting that deliberate optimization of affinity could be a key to fully harnessing the therapeutic potential of ADC *in vivo*. CD276-8 ADC thus represents a promising therapeutic candidate for patients with B7-H3-expressing solid tumors, warranting further investigation into its safety and mechanisms of action.

Supplementary Materials: The following supporting information can be downloaded at the website of this paper posted on Preprints.org, Figure S1: Binding affinity curves of CD276-3, CD276-8, DS7300 against human B7-H3; Figure S2: The epitope grouping of CD276-3, CD276-8 and DS7300 determined by BLI; Figure S3: Characterization of CD276-3 ADC, CD276-8 ADC, DS7300 ADC (DAR8), DS7300 ADC (DAR4) and isotype ADC; Figure S4: The developability of CD276-8 and thermal stability of CD276-8 and CD276-8 ADC.

Author Contributions: Conceptualization, J.Z., H.Z., and Z.Z.; Molecular discovery, S.W.; In vitro assays, Z.Z., H.Z, Z.L., and S.W.; Animal experiments, Z.Z. and H.Z.; Data analysis, Z.Z., H.Z., and Z.L.; Writing-original draft, Z.Z., J.Z., H.Z.; Writing-review & editing, Z.Z., J.Z., H.Z., X.X., Y.X., S.W. and Z.L. All authors have read and agreed to the published version of the manuscript.

Funding: This research was supported by National Natural Science Foundation of China, Grant No. 81773621 and 82073751 to JWZ, and the National Science and Technology Major Project "Key New Drug Creation and Manufacturing Program" of China, Grant No.2019ZX09732001-019 to JWZ.

Institutional Review Board Statement: All mice were housed in isolated ventilated cages barrier facility at Shanghai Jiao Tong University Laboratory Animal Center. The mice were maintained on a 12/12-hour light/dark cycle, 20-26℃ with sterile pellet food and water ad libitum. The animal study was performed in accordance with the recommendations in the Guide for the Care and Use of Laboratory Animals and relevant Chinese laws and regulations. The protocol was approved by the Institutional Animal Care and Use Committee (IACUC) of Shanghai Jiao Tong University.

Informed Consent Statement: Not applicable.

Data Availability Statement: The original contributions presented in this study are included in the article and supplementary material. Further inquiries can be directed to the corresponding author(s).

Acknowledgments: We thank Jecho Laboratories and Jecho Institute for their valuable technical support in molecule discovery, antibody expression and purification, and stability analysis. We are also thankful to Yuanyuan Zhu and Huifang Liu from Instrumental Analysis Center, Shanghai Jiao Tong University for their valuable technical support in LC-MS analysis.

Conflicts of Interest: The authors declare no conflicts of interest.

Abbreviations

The following abbreviations are used in this manuscript:

ADC	Antibody-drug Conjugate
BLI	Bio-Layer Interferometry
HCA	High Content Analysis
CDX	Cell line-derived xenograft
IgC	Immunoglobulin constant-like domain
IgV	Immunoglobulin variable-like domain
NSCLC	Non-Small Cell Lung Cancer
IHC	Immunohistochemistry

 doi:10.20944/preprints202602.0621.v1

TME	Tumor Microenvironment
ADCC	Antibody-Dependent Cellular Cytotoxicity
mAb	Monoclonal Antibody
TCE	T-Cell Engager
CAR-T	Chimeric Antigen Receptor-T cells
TOP1	Topoisomerase I
DAR	Drug-to-Antibody Ratio
SEC-HPLC	Size Exclusion Chromatography
RP-HPLC	Reversed-Phase High-Performance Liquid Chromatography
PK	Pharmacokinetic
CDR	Complementarity Determining Region
FACS	Fluorescence Activated Cell Sorting
MFI	Mean Fluorescence Intensity
CTG	CellTiter-Glo
IC_{50}	The Half Maximal Inhibitory Concetration
BLQ	Below Lower Limit of Quantification
TGI	Tumor Growth Inhibition
SMAC-HPLC	Standup Monolayer Adsorption Chromatography
CIC-HPLC	Cross Interaction Chromatography
DSF	Differential Scanning Fluorimetry
T_m	Melting Point
AS	Accelerated Stability
F/T	Freeze-Thawing
PBS	Phosphate Buffered Saline
WCX-HPLC	Weak Cation Exchange Chromatography
MES	2-Morpholinoethanesulphonic acid
TFA	Trifluoroacetic Acid
HPA	Human Protein Atlas
SEM	Standard Error of Mean
RT	Retention Time
EC_{50}	Concentration for 50% of Maximal Effect

References

1. Schildberg, F.A.; Klein, S.R.; Freeman, G.J.; Sharpe, A.H. Coinhibitory Pathways in the B7-CD28 Ligand-Receptor Family. *Immunity* **2016**, *44*, 955-972, doi:10.1016/j.immuni.2016.05.002.
2. Seaman, S.; Zhu, Z.; Saha, S.; Zhang, X.M.; Yang, M.Y.; Hilton, M.B.; Morris, K.; Szot, C.; Morris, H.; Swing, D.A.; et al. Eradication of Tumors through Simultaneous Ablation of CD276/B7-H3-Positive Tumor Cells and Tumor Vasculature. *Cancer Cell* **2017**, *31*, 501-515 e508, doi:10.1016/j.ccell.2017.03.005.
3. Zhang, X.; Guo, H.; Chen, J.; Xu, C.; Wang, L.; Ke, Y.; Gao, Y.; Zhang, B.; Zhu, J. Highly proliferative and hypodifferentiated CAR-T cells targeting B7-H3 enhance antitumor activity against ovarian and triple-negative breast cancers. *Cancer Lett* **2023**, *572*, 216355, doi:10.1016/j.canlet.2023.216355.
4. Picarda, E.; Ohaegbulam, K.C.; Zang, X. Molecular Pathways: Targeting B7-H3 (CD276) for Human Cancer Immunotherapy. *Clinical Cancer Research* **2016**, *22*, 3425-3431, doi:10.1158/1078-0432.Ccr-15-2428.
5. Yamato, I.; Sho, M.; Nomi, T.; Akahori, T.; Shimada, K.; Hotta, K.; Kanehiro, H.; Konishi, N.; Yagita, H.; Nakajima, Y. Clinical importance of B7-H3 expression in human pancreatic cancer. *Br J Cancer* **2009**, *101*, 1709-1716, doi:10.1038/sj.bjc.6605375.
6. Inamura, K.; Yokouchi, Y.; Kobayashi, M.; Sakakibara, R.; Ninomiya, H.; Subat, S.; Nagano, H.; Nomura, K.; Okumura, S.; Shibutani, T.; et al. Tumor B7-H3 (CD276) expression and smoking history in relation to lung adenocarcinoma prognosis. *Lung Cancer* **2017**, *103*, 44-51, doi:10.1016/j.lungcan.2016.11.013.
7. Luo, L.; Zhu, G.; Xu, H.; Yao, S.; Zhou, G.; Zhu, Y.; Tamada, K.; Huang, L.; Flies, A.D.; Broadwater, M.; et al. B7-H3 Promotes Pathogenesis of Autoimmune Disease and Inflammation by Regulating the Activity of Different T Cell Subsets. *PLoS One* **2015**, *10*, e0130126, doi:10.1371/journal.pone.0130126.
8. Zhou, X.; Ouyang, S.; Li, J.; Huang, X.; Ai, X.; Zeng, Y.; Lv, Y.; Cai, M. The novel non-immunological role and underlying mechanisms of B7-H3 in tumorigenesis. *J Cell Physiol* **2019**, *234*, 21785-21795, doi:10.1002/jcp.28936.

 doi:10.20944/preprints202602.0621.v1

9. Getu, A.A.; Tigabu, A.; Zhou, M.; Lu, J.; Fodstad, Ø.; Tan, M. New frontiers in immune checkpoint B7-H3 (CD276) research and drug development. *Molecular Cancer* **2023**, *22*, doi:10.1186/s12943-023-01751-9.
10. Hafeez, U.; Parakh, S.; Gan, H.K.; Scott, A.M. Antibody-Drug Conjugates for Cancer Therapy. *Molecules* **2020**, *25*, doi:10.3390/molecules25204764.
11. Zong, H.F.; Li, X.; Han, L.; Wang, L.; Liu, J.J.; Yue, Y.L.; Chen, J.; Ke, Y.; Jiang, H.; Xie, Y.Q.; et al. A novel bispecific antibody drug conjugate targeting HER2 and HER3 with potent therapeutic efficacy against breast cancer. *Acta Pharmacol Sin* **2024**, *45*, 1727-1739, doi:10.1038/s41401-024-01279-8.
12. Min, Y.; Chen, Y.; Wang, L.; Ke, Y.; Rong, F.; He, Q.; Paerhati, P.; Zong, H.; Zhu, J.; Wang, Y.; et al. Supramolecular antibody-drug conjugates for combined antibody therapy and photothermal therapy targeting HER2-positive cancers. *Int J Biol Macromol* **2024**, *278*, 134622, doi:10.1016/j.ijbiomac.2024.134622.
13. Feng, Y.; Lee, J.; Yang, L.; Hilton, M.B.; Morris, K.; Seaman, S.; Edupuganti, V.; Hsu, K.S.; Dower, C.; Yu, G.; et al. Engineering CD276/B7-H3-targeted antibody-drug conjugates with enhanced cancer-eradicating capability. *Cell Rep* **2023**, *42*, 113503, doi:10.1016/j.celrep.2023.113503.
14. Siena, S.; Di Bartolomeo, M.; Raghav, K.; Masuishi, T.; Loupakis, F.; Kawakami, H.; Yamaguchi, K.; Nishina, T.; Fakih, M.; Elez, E.; et al. Trastuzumab deruxtecan (DS-8201) in patients with HER2-expressing metastatic colorectal cancer (DESTINY-CRC01): a multicentre, open-label, phase 2 trial. *Lancet Oncol* **2021**, *22*, 779-789, doi:10.1016/S1470-2045(21)00086-3.
15. Bardia, A.; Jhaveri, K.; Kalinsky, K.; Pernas, S.; Tsurutani, J.; Xu, B.; Hamilton, E.; Im, S.A.; Nowecki, Z.; Sohn, J.; et al. TROPION-Breast01: Datopotamab deruxtecan vs. chemotherapy in pre-treated inoperable or metastatic HR+/HER2- breast cancer. *Future Oncol* **2024**, *20*, 423-436, doi:10.2217/fon-2023-0188.
16. Nagase-Zembutsu, A.; Hirotani, K.; Yamato, M.; Yamaguchi, J.; Takata, T.; Yoshida, M.; Fukuchi, K.; Yazawa, M.; Takahashi, S.; Agatsuma, T. Development of DS-5573a: A novel afucosylated mAb directed at B7-H3 with potent antitumor activity. *Cancer Sci* **2016**, *107*, 674-681, doi:10.1111/cas.12915.
17. Masuda, T.; Naito, H.; Nakada, T.; Yoshida, M.; Ashida, S.; Miyazaki, H.; Kasuya, Y.; Morita, K.; Abe, Y.; Ogitani, Y. Antibody-drug conjugate. US11633493B2, 2020.
18. Lyon, R.P.; Meyer, D.L.; Setter, J.R.; Senter, P.D. Conjugation of anticancer drugs through endogenous monoclonal antibody cysteine residues. *Methods Enzymol* **2012**, *502*, 123-138, doi:10.1016/B978-0-12-416039-2.00006-9.
19. Ji, A.; Sun, C.; He, W. Process for preparing antibody-drug conjugates with improved homogeneity for use in treating cancer, autoimmune, and infective disorders. WO2020164561, 2020.
20. Matsuda, Y.; Leung, M.; Tawfiq, Z.; Fujii, T.; Mendelsohn, B.A. In-situ Reverse Phased HPLC Analysis of Intact Antibody-Drug Conjugates. *Anal Sci* **2021**, *37*, 1171-1176, doi:10.2116/analsci.20P424.
21. Wang, L.; Ke, Y.; He, Q.; Paerhati, P.; Zhuang, W.; Yue, Y.; Liu, J.; Zhang, J.; Huang, L.; Yin, Q.; et al. A novel ROR1-targeting antibody-PROTAC conjugate promotes BRD4 degradation for solid tumor treatment. *Theranostics* **2025**, *15*, 1238-1254, doi:10.7150/thno.102531.
22. Pei, M.; Liu, T.; Ouyang, L.; Sun, J.; Deng, X.; Sun, X.; Wu, W.; Huang, P.; Chen, Y.L.; Tan, X.; et al. Enzyme-linked immunosorbent assays for quantification of MMAE-conjugated ADCs and total antibodies in cynomolgus monkey sera. *J Pharm Anal* **2022**, *12*, 645-652, doi:10.1016/j.jpha.2021.11.005.
23. Wei, C.; Zhang, G.; Clark, T.; Barletta, F.; Tumey, L.N.; Rago, B.; Hansel, S.; Han, X. Where Did the Linker-Payload Go? A Quantitative Investigation on the Destination of the Released Linker-Payload from an Antibody-Drug Conjugate with a Maleimide Linker in Plasma. *Anal Chem* **2016**, *88*, 4979-4986, doi:10.1021/acs.analchem.6b00976.
24. Zhang, Y.; Huo, M.; Zhou, J.; Xie, S. PKSolver: An add-in program for pharmacokinetic and pharmacodynamic data analysis in Microsoft Excel. *Comput Methods Programs Biomed* **2010**, *99*, 306-314, doi:10.1016/j.cmpb.2010.01.007.
25. Kohli, N.; Jain, N.; Geddie, M.L.; Razlog, M.; Xu, L.; Lugovskoy, A.A. A novel screening method to assess developability of antibody-like molecules. *MAbs* **2015**, *7*, 752-758, doi:10.1080/19420862.2015.1048410.
26. Hedberg, S.H.M.; Rapley, J.; Haigh, J.M.; Williams, D.R. Cross-interaction chromatography as a rapid screening technique to identify the stability of new antibody therapeutics. *Eur J Pharm Biopharm* **2018**, *133*, 131-137, doi:10.1016/j.ejpb.2018.10.009.

 doi:10.20944/preprints202602.0621.v1

27. Okajima, D.; Yasuda, S.; Maejima, T.; Karibe, T.; Sakurai, K.; Aida, T.; Toki, T.; Yamaguchi, J.; Kitamura, M.; Kamei, R.; et al. Datopotamab Deruxtecan, a Novel TROP2-directed Antibody-drug Conjugate, Demonstrates Potent Antitumor Activity by Efficient Drug Delivery to Tumor Cells. *Mol Cancer Ther* **2021**, *20*, 2329-2340, doi:10.1158/1535-7163.MCT-21-0206.
28. Yamato, M.; Hasegawa, J.; Maejima, T.; Hattori, C.; Kumagai, K.; Watanabe, A.; Nishiya, Y.; Shibutani, T.; Aida, T.; Hayakawa, I.; et al. DS-7300a, a DNA Topoisomerase I Inhibitor, DXd-Based Antibody-Drug Conjugate Targeting B7-H3, Exerts Potent Antitumor Activities in Preclinical Models. *Mol Cancer Ther* **2022**, *21*, 635-646, doi:10.1158/1535-7163.MCT-21-0554.
29. Ogitani, Y.; Aida, T.; Hagihara, K.; Yamaguchi, J.; Ishii, C.; Harada, N.; Soma, M.; Okamoto, H.; Oitate, M.; Arakawa, S.; et al. DS-8201a, A Novel HER2-Targeting ADC with a Novel DNA Topoisomerase I Inhibitor, Demonstrates a Promising Antitumor Efficacy with Differentiation from T-DM1. *Clin Cancer Res* **2016**, *22*, 5097-5108, doi:10.1158/1078-0432.CCR-15-2822.
30. Goyon, A.; Excoffier, M.; Janin-Bussat, M.C.; Bobaly, B.; Fekete, S.; Guillarme, D.; Beck, A. Determination of isoelectric points and relative charge variants of 23 therapeutic monoclonal antibodies. *J Chromatogr B Analyt Technol Biomed Life Sci* **2017**, *1065-1066*, 119-128, doi:10.1016/j.jchromb.2017.09.033.
31. Bailly, M.; Mieczkowski, C.; Juan, V.; Metwally, E.; Tomazela, D.; Baker, J.; Uchida, M.; Kofman, E.; Raoufi, F.; Motlagh, S.; et al. Predicting Antibody Developability Profiles Through Early Stage Discovery Screening. *MAbs* **2020**, *12*, 1743053, doi:10.1080/19420862.2020.1743053.
32. Weng, W.; Meng, T.; Zhao, Q.; Shen, Y.; Fu, G.; Shi, J.; Zhang, Y.; Wang, Z.; Wang, M.; Pan, R.; et al. Antibody-Exatecan Conjugates with a Novel Self-immolative Moiety Overcome Resistance in Colon and Lung Cancer. *Cancer Discov* **2023**, *13*, 950-973, doi:10.1158/2159-8290.CD-22-1368.
33. Calopiz, M.C.; Linderman, J.J.; Thurber, G.M. Optimizing Solid Tumor Treatment with Antibody-drug Conjugates Using Agent-Based Modeling: Considering the Role of a Carrier Dose and Payload Class. *Pharm Res* **2024**, *41*, 1109-1120, doi:10.1007/s11095-024-03715-0.
34. Tsumura, R.; Manabe, S.; Takashima, H.; Koga, Y.; Yasunaga, M.; Matsumura, Y. Influence of the dissociation rate constant on the intra-tumor distribution of antibody-drug conjugate against tissue factor. *J Control Release* **2018**, *284*, 49-56, doi:10.1016/j.jconrel.2018.06.016.
35. Trail, P. Antibody Drug Conjugates as Cancer Therapeutics. *Antibodies* **2013**, *2*, 113-129, doi:10.3390/antib2010113.
36. Li, S.; Zhang, M.; Wang, M.; Wang, H.; Wu, H.; Mao, L.; Zhang, M.; Li, H.; Zheng, J.; Ma, P.; et al. B7-H3 specific CAR-T cells exhibit potent activity against prostate cancer. *Cell Death Discov* **2023**, *9*, 147, doi:10.1038/s41420-023-01453-7.